Proceedings of the 11th Brazilian Congress of Thermal Sciences and Engineering -- ENCIT 2006
Braz. Soc. of Mechanical Sciences and Engineering -- ABCM, Curitiba, Brazil,- Dec. 5-8, 2006

Paper CIT06-0481

AN OVERVIEW OF HIGH-RESOLUTION SCHEMES FOR AEROACOUSTICS

Odenir de Almeida
EMBRAER – Empresa Brasileira de Aeronáutica S.A
Av. Brigadeiro Faria Lima, 2170 – São José dos Campos - SP
odenir.almeida@embraer.com.br

Francisco José de Souza
EMBRAER – Empresa Brasileira de Aeronáutica S.A
Av. Brigadeiro Faria Lima, 2170 – São José dos Campos - SP
francisco.souza@embraer.com.br

Abstract. *The present work can be conceived as a first step in the direction of constructing an aeroacoustic solver. Such development in Computational Aeroacoustics (CAA) is not achieved before a complete understanding of the physics involved in acoustic problems. Thus a brief technical background in CAA is presented in order to introduce the numerical activities performed herein. The one-dimensional wave equation has been discretized with optimized high order finite difference schemes taking into consideration usual conditions of consistency, stability and convergence. These schemes are known as DRP (Dispersion-Relation-Preserving). To advance the solution in time, high order Runge-Kutta schemes are applied. In order to validate the numerical scheme, initial disturbance functions are used, which are propagated in a 1D mesh. The advantages and limitations for the numerical schemes are deeply discussed shedding light to the relevant parameters which are necessary to achieve a good aeroacoustic simulation. The numerical results generated in this work are compared with the exact analytical solutions showing a good agreement.*

Keywords*. Aeroacoustics, wave-equation, finite difference, numerical schemes, aerodynamic noise*

1. Introduction

Computational aeroacoustics (CAA) has made impressive progress along the last decades. Most of this advance has been driven by car aerodynamics and essentially aircraft designs for low noise. From the dawn of Sir James Lighthill work in 1952 up to recent days, aeroacoustic has evolved in terms of acquired knowledge about physical phenomena and development of tools for academic and industrial applications. Indeed, it cannot be neglected that many classes of acoustic problems were completely understood and solved by analytical and numerical approaches so far. Also, it is important to emphasize that these acoustic problems are essentially canonical cases involving wave propagation in very simple domains. With the need for industrial application of CAA in the last decade, numerical efforts have been specially concentrated in the creation of tools aimed to predict the generation and propagation of aerodynamic sound.

The following discussion has been addressed by some authors in the literature and consists of an important key about separating classical computational fluid dynamics (CFD) of the recent CAA. In essence, it is important to keep in mind that classical CFD simulations cannot handle acoustic phenomena.

Differently from a classic computational fluid dynamics (CFD) analysis, there are other important physical and numerical issues related to computational aeroacoustics. From the physical standpoint, it is largely known that sound is most generated by transitional and turbulent flow phenomena like separation and shearing, vortex shedding, impingement and shocks. In all these cases there are a wide range of length and time scales associated. In the flow field these length and time scales are quite different from those ones existing in the acoustic field. Figure 1 illustrates the length and time scales difference between fluid mechanic and acoustic. Kolmogorov's scales (δ) of turbulence are much smaller than the wavelength (λ) of the generated sound waves which by it's turn is smaller than the characteristic fluid dynamic length or the largest eddy in the flow field (L).

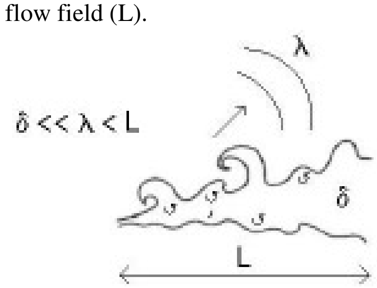

Figure 1. Disparity between the flow field and acoustic scales.

It's important to remember that for aerodynamics or fluid mechanic problems, flow disturbances, generally, tend to decay very fast away from a body or their source of generation. That is, any flow disturbance suffers the effects of dispersion and dissipation along the flow field. On the other hand, acoustic waves are non-dispersive and non-dissipative and consequently decay very slowly in the acoustic field, traveling for long distances until reaching any observer. From the numerical standpoint, such physical implications listed above drive numerical requirements like dealing with different length scales in different parts of the computational domain. Yet, numerical schemes used to evaluate time and space-derivatives should be of low dispersion and dissipation error in order to guarantee long wave propagations. Another limiter is the computation domain that is inevitably finite in size. Thus, acoustic waves being propagated decay very slowly and actually reach the boundaries of the computation domain. To avoid the reflection of outgoing sound waves back into the computation domain and contamination of the solution, radiation and outflow boundary conditions must be imposed at the artificial exterior boundaries to assist the waves to exit smoothly. And finally, still considering a finite domain, the wave propagation needs to be performed outside of the computational domain to reach an observed that is often far away from the sound source generation. The discretization of such big domain is completely out of question and so, numerical propagation methodologies should deal with this problem.

According to Tam (2005), the need for highly accurate numerical methods was recognized from the earliest stages in the development of Computational Aeroacoustics (CAA) since the classical computational fluid dynamics could not deal with long-time integration with minimal dissipation and dispersion in order to guarantee the propagation of sound waves in the far-field.

As a summary presented by Tam (2004) to simulate an aeroacoustic phenomenon or problem computationally, the numerical algorithm must consist of several basic elements which are listed below:

(1) A time marching computation scheme;

(2) A suitably designed computation grid;

(3) An artificial selective damping algorithm or filtering procedure if the marching scheme has no built-in artificial selective damping;

(4) A set of radiation/outflow numerical treatments for use at the boundaries of the computation domain.

Along the years, different methodologies have been created and applied to build aeroacoustic numerical codes. It started with the use of higher order schemes by believing that they were more suitable than lower-order schemes in terms of stability. For acoustic calculations, however, the stability consideration alone is not sufficient, since Runge-Kutta schemes retail both dissipation and dispersion errors. The numerical solutions need to be also time accurate to resolve the wave propagations. Time integration has then been optimized with the same aim in view, especially using Runge–Kutta (RK) algorithms – Berland (2005).

By reviewing the literature and seeking for low-dissipative, low-dispersive and large spectral bandwidth numerical algorithms it can be found relevant works in aeroacoustics. For instance, Tam & Webb (1993b) exploited the DRP (Dispersion-Relation-Preserving) schemes, Lele (1992) developed compact finite differences, and recently Bogey & Bailly (2004) built up explicit finite differences and selective filters accurate for waves down to four points per wavelength.

Other numerical works as of Roeck *et al* (2004), Tam (2004), have presented high-order finite difference schemes for computational aeroacoustics. However, when dealing with space and time derivatives discretization, special attention should be given to DRP schemes which in essence possess the same dispersion relations as the original partial differential equations. As presented by Tam & Webb (1993a) the central idea of this approach is that a time marching high order finite difference scheme can faithfully reproduce the three types of waves, namely the acoustic, vorticity, and entropy waves, of the linearized Euler equations. Nevertheless, this is only true if the dispersion relations of the finite difference scheme are the same as those of the partial differential equations. In terms of numerical results, the DRP schemes tend to be more suitable for wave solutions. The complete description of these schemes can be found in the work of Tam & Webb (1993b). However, it is important to emphasize that the main focus of the work presented herein is given to the exploration of DRP (Dispersion-Relation-Preserving) spatial schemes.

In general, the present work can be divided in two objectives. The first one is to provide a general overview about computational aeroacoustic requirements through the discussion of some relevant associated issues and by presenting recommended references to those ones that are initiating researches in this area. The second objective is to present the validation of time and spatial discretization of the wave equation by using different schemes and focusing on the use of DRP schemes. To accomplish this task, numerical simulations for the propagation of a pulse or disturbance are conducted. The solution is compared with analytical results showing a good agreement. Finally, the advantages and limitations for the numerical schemes are deeply discussed shedding light to the relevant parameters which are necessary to achieve a good aeroacoustic simulation.

2. Numerical Schemes

This section is aimed to provide a general guidance about numerical schemes that can be used for aeroacoustic simulations. The focus will be given to DRP schemes for spatial discretization and Runge-Kutta time integration methods which will be summarized and presented hereafter.

Standard central differences schemes are presented in Roeck *et al* (2004), in which a spatial derivative of a function in a grid point is approximated by a weighted summation of the function values in the neighboring grid points. For a 7-point (ST7) and 9-point (ST9) stencil, a 6^{th} and an 8^{th} order accurate scheme, respectively, is obtained.

With the same approach of improving the dissipation and dispersion characteristics, other works were proposed (e.g. Bogey *et al.* (2002), Hu *et al.* (1996) and Lele (1992)). The importance of dispersion relations of the finite difference schemes have been emphasized in these works with good results in terms of wave propagation and robustness of the computation.

In this context, the low-dispersion and low-dissipation numerical schemes also known as DRP (Dispersion-relation-preserving) presented by Tam & Webb (1993b) seems to be one of the most suitable for aeroacoustic problems. Tam (1993b, 2004) has discussed the numerical issues related to these schemes.

Regarding temporal discretization the most common methods are the Runge-Kutta schemes. These methods have been evolved following the same idea of DRP schemes, where dispersion and dissipation of the scheme are minimized in the Fourier space over a large range of frequencies for linear operators, as presented by Hu et al. (1996) and Bogey and Bailly (2003).

In the following section, a brief description of these schemes is presented and discussed. The numerical implementation was concentrated in the DRP 7-point, DRP 15-point schemes of Tam & Webb (1993b) and Tam (2004), respectively, and the 9-point optimized central difference scheme of Bogey et al. (2002). For time integration two Runge-Kutta schemes were selected based on independent criteria of low-storage (Williamson (1980)) and low-dispersion/dissipation (Hu et al (1996)).

In summary, the understanding and numerical implementation of these schemes could be considered an initial step in order to build an aeroacoustic solver which is the main goal for work future.

2.1. Spatial Discretization

The description of optimized spatial discretization for the Dispersion-Relation-Preserving (DRP) schemes is given in the work of Tam & Webb (1993b) as follows:

Consider the approximation of the first derivative $\partial f / \partial x$ - Equation (1) at the *l*th node of a uniform grid. Suppose *M* values of *f* to the right and *N* values of *f* to the left of this point are used to form the finite difference approximation – Figure 2.

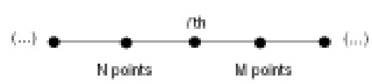

Figure 2. Uniform grid representation.

$$\left(\frac{\partial f}{\partial x}\right)_i \approx \frac{1}{\Delta x}\sum_{j=-N}^{M} a_j f_{l+j} \tag{1}$$

The usual procedure is to expand the right-hand side of (1) in Taylor series of Δx and then determine the coefficients a_j by equating coefficients of the same powers of Δx. Finite difference schemes constructed in this way will be referred to as the standard schemes. In the DRP schemes the coefficients a_j are found in a different way. It is proposed that they be determined by requiring the Fourier transform of the finite difference scheme on the right of (1) to be a close approximation of that of the partial derivative on the left.

The finite difference equation (1) is a special case of the following equation in which *x* is a continuous variable:

$$\frac{\partial f}{\partial x}(x) \approx \frac{1}{\Delta x}\sum_{j=-N}^{M} a_j f(x + j\Delta x) \tag{2}$$

(1) can be recovered from (2) by setting $x = l\Delta x$. The Fourier transform and its inverse of a function are related by

$$\tilde{f}(\alpha)=\frac{1}{2\pi}\int_{-\infty}^{\infty} f(x)e^{-i\alpha x}dx \tag{3}$$

$$f(x)=\int_{-\infty}^{\infty}\tilde{f}(\alpha)e^{i\alpha x}d\alpha \tag{4}$$

The Fourier transform of the left and right sides of (2) are:

$$i\alpha\tilde{f}\approx\left(\frac{1}{\Delta x}\sum_{j=-N}^{M}a_j e^{i\alpha j\Delta x}\right)\tilde{f} \tag{5}$$

by comparing the two sides of (5) it is clear that the quantity

$$\overline{\alpha}=\frac{-i}{\Delta x}\sum_{j=-N}^{M}a_j e^{ij\alpha\Delta x} \tag{6}$$

is effectively the wave number of the Fourier transform of the finite difference scheme (2) or (1); $\overline{\alpha}\Delta x$ is a periodic function of $\alpha\Delta x$ with period 2π. To assure that the Fourier transform of the finite difference scheme is a good approximation of that of the partial derivative over the range of wave numbers of interest (waves with wave length longer than four Δx or $|\alpha\Delta x|<\pi/2$ it is required that a_j be chosen to minimize the integrated error *E* defined:

$$E=\int_{-\pi/2}^{\pi/2}\left|\alpha\Delta x-\overline{\alpha}\Delta x\right|^2 d(\alpha\Delta x) \tag{7}$$

$$=\int_{-\pi/2}^{\pi/2}\left|ik-\sum_{j=-N}^{M}a_j e^{ijk}\right|^2 dk \tag{8}$$

The conditions that *E* is a minimum are

$$\frac{\partial E}{\partial a_j}=0\text{, } j=-N \text{ to } M; \tag{9}$$

(9) provides a system of linear algebraic equations by which the coefficients a_j can be easily determined.
More details about DRP schemes can be found in Tam & Webb (1993b).
The coefficients of the 7-point and 15-point DRP schemes used in this work are:

7-point scheme:

$a_0 = 0$

$a_1 = -a_1 =$ 0.77088238051822552

$a_2 = -a_2 =$ -0.166705904414580469

$a_3 = -a_3 =$ 0.02084314277031176

15-point scheme:

$a_0 = 0$

$a_1 = -a_1 =$ 0.91942501110343045059277722885

$a_2 = -a_2 =$ -0.35582959926835268755667642401

$a_3 = -a_3 =$ 0.15251501608406492469104928679

a4 = -a4 = -0.059463040829715772666828596899

a5 = -a5 = 0.019010752709508298659849167988

a6 = -a6 = -0.0043808649297336481851137000907

a7 = -a7 = 0.00053896121868623384659692955878

Artificial Selective Damping:

To obtain a high-quality numerical solution, it is necessary to eliminate the short wavelength spurious numerical waves. The origin of these spurious waves is related to grid-to-grid oscillations and a way to eliminate or reduce such instabilities is introducing artificial selective damping terms in the finite difference equations. Tam & Webb (1993b) used tailored damping terms specifically for eliminating only the short waves without affecting the physical long waves.

Additional information about this approach can also be found in Roeck *et al* (2004) and Bogey and Bailly (2004). The present work considers both the effect of the artificial selective damping as described in Tam & Webb (1993b) and no use of selective damping. The artificial selective damping has been applied only for the DRP scheme. The coefficients for the damping function are given as follows:

$c_0 = 0.3276986608$

c1 = -c1 = -0.235718815

c2 = -c2 = 0.0861506696

c3 = -c3 = -0.0142811847

2.2. Time Integration

Runge-Kutta algorithms are largely used in fluid dynamics applications because stability over a wide range of frequencies. Many of these algorithms were optimized for low-storage requirements in order to make easier the numerical computation on systems that are very large. A good reference in this area is the work of Williamson (1980) where low-storage schemes up to fourth order were evaluated without losing stability and accuracy.

According to Hu et al. (1996) for computing acoustic waves, only the stability consideration is not sufficient, since the Runge-Kutta schemes also entail both dissipation and dispersion errors. Many works go to the direction of optimizing Runge-Kutta schemes for low dispersion and dissipation properties. This is the case of works from Hu et al. (1996) and Bogey and Bailly (2004).

In order to present a summary of the approach done herein, let the time evolution equation be written as follows:

$$\frac{\partial U}{\partial t} = F(U) \qquad (10)$$

in which U represents the vector containing the solution values at the spatial mesh points and the operator F contains the discretization of the spatial derivatives. For simplicity, it's assumed that F does not depend on t explicitly. An explicit low storage p-stage Runge-Kutta scheme advances the solution from time level t_n to $t_n + \Delta t$ as:

$$\begin{aligned} u^0 &= u^n \\ u^l &= u^n + \alpha_l \Delta t F(u^{l-1}) \qquad \text{for } l = 1,\ldots,p \\ u^{n+1} &= u^p \end{aligned} \qquad (11)$$

The standard p-stage Runge-Kutta schemes of pth-order (for a linear operator F) can be obtained with Taylor Series expansion of $u(t_n + \Delta t)$. The coefficients α_j should be chosen to obey several conditions as maximum order of accuracy. Like the spatial integration, presented in section 2.1, the coefficients α_j can also be chosen to minimize the dispersion and dissipation errors.

More details about the determination of these coefficients can be found in Hu et al. (1996), Roeck (2004) and Berland *et al.* (2005). In this paper, the low-storage and low-dispersion/dissipation properties are evaluated through the implementation of the following Runge-Kutta schemes:

- 3rd order low-storage Runge-Kutta scheme – Williamson (1980) – RK3W
- 5 stages low-dissipation and low-dispersion 2nd order Runge-Kutta scheme – Hu et al (1996) – LLDRK5
- 5 stages 2nd order optimized Runge-Kutta scheme – Bogey and Bailly (2002) – RKO5

The coefficients α_j for the schemes of Hu et al (1996) and Bogey and Bailly (2002) are written in Table 1.

Table 1 - α_j for RK5 and RK6

	α_1	α_2	α_3	α_4	α_5	α_6
LLDRK5	0.197707993	0.237179241	0.333116	0.5	1	-
RKO5	0.181575486	0.238260222	0.330500707	0.5	1	-

3. Validation problem

To validate the scheme properties, two initial value problem of a one-dimensional convective wave equation are considered.

The mathematical problem consists in finding the solution for the wave equation:

$$\frac{\partial u}{\partial t}+\frac{\partial u}{\partial x}=0 \tag{12}$$

with an initial disturbance $u=f(x)$ at time $t=0$. The solution consists of the initial disturbance propagating to the right in an one-dimensional mesh. The propagation of this disturbance posses a dimensionless speed equal to 1 ($u=f(x-t)$).

The initial disturbance functions $f(x)$ used in this work are described below:

(1) Box-car function:

$$t=0, \qquad f(x)=0.5[H(x+50)-H(x-50)] \tag{13}$$

The factor 0.5 defines the amplitude of the step function and 50 is the haft width of the box-car. The fourier transformation of this function contains high frequency components and these must be damped in order to avoid spurious high-frequency waves. For this reason, this function is a good way to evaluate the effect of artificial damping.

(2) Gaussian function:

$$t=0, \qquad f(x)=0.5\exp\left[-\ln 2\left(\frac{x}{3}\right)^2\right] \tag{14}$$

According to Roeck (2004) the Gaussian function is used to evaluate the general dispersion and dissipation properties and the stability ranges of the scheme. The Fourier transformation of a Gaussian pulse is also a Gaussian pulse with a maximum at $k\Delta x=0$. The initial disturbance will therefore be mainly situated in the long wave range and artificial damping is not necessary and will not be added to the numerical scheme.

The variables of equation (12) are made dimensionless with Δx as length scale and $\Delta x/c_0$ as the time scale. The computational domains have a dimensionless length of 700 Δx for the Gaussian and Box-car functions.

Figure 3 presents the analytical solution for the functions (1) and (2) at the initial time ($t=0$).

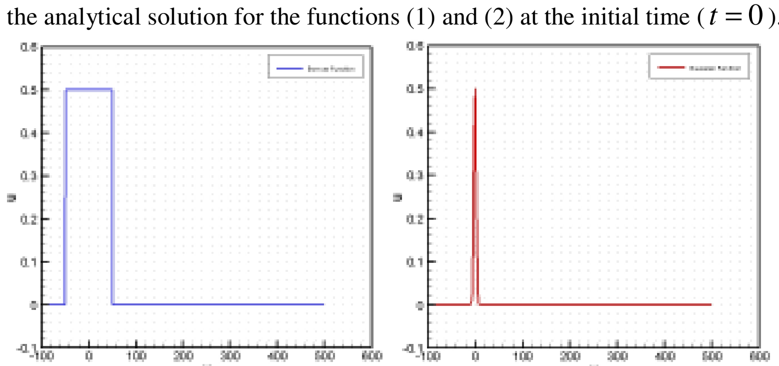

Figure 3. Analytical solution for the functions (1) and (2) at the initial time ($t=0$).

All the calculations were done with a grid spacing Δx equal to unity and a time step Δt equal to 0.1. The stability requirements were satisfied with a CFL ($\Delta t / \Delta x$) of 0.1.

In this work it's not applied any kind of boundary conditions. The simulations were evaluated for a dimensionless time of 400. At this time, the initial disturbance reaches the dimensionless position of 400. Taking this into account, no specific boundary conditions have been added since spurious reflections of the initial disturbance at the boundaries are negligible if the disturbance has not reached the boundary yet.

4. Results

4.1 Initial Disturbance Function - Box-car Function

Figure 4 shows the computed results of the seven-point DRP scheme with different Runge-Kutta time integration methods. For these results damping was not used. For comparison purposes, the analytical solution is plotted against the numerical results.

The presence of spurious waves is evident in the computed solution. These spurious waves are generated by the discontinuities of the initial condition and due to grid-to-grid oscillations. The Runge-Kutta schemes were quite stable for all simulations and it's possible to say that all the numerical error was introduced by the spatial discretization.

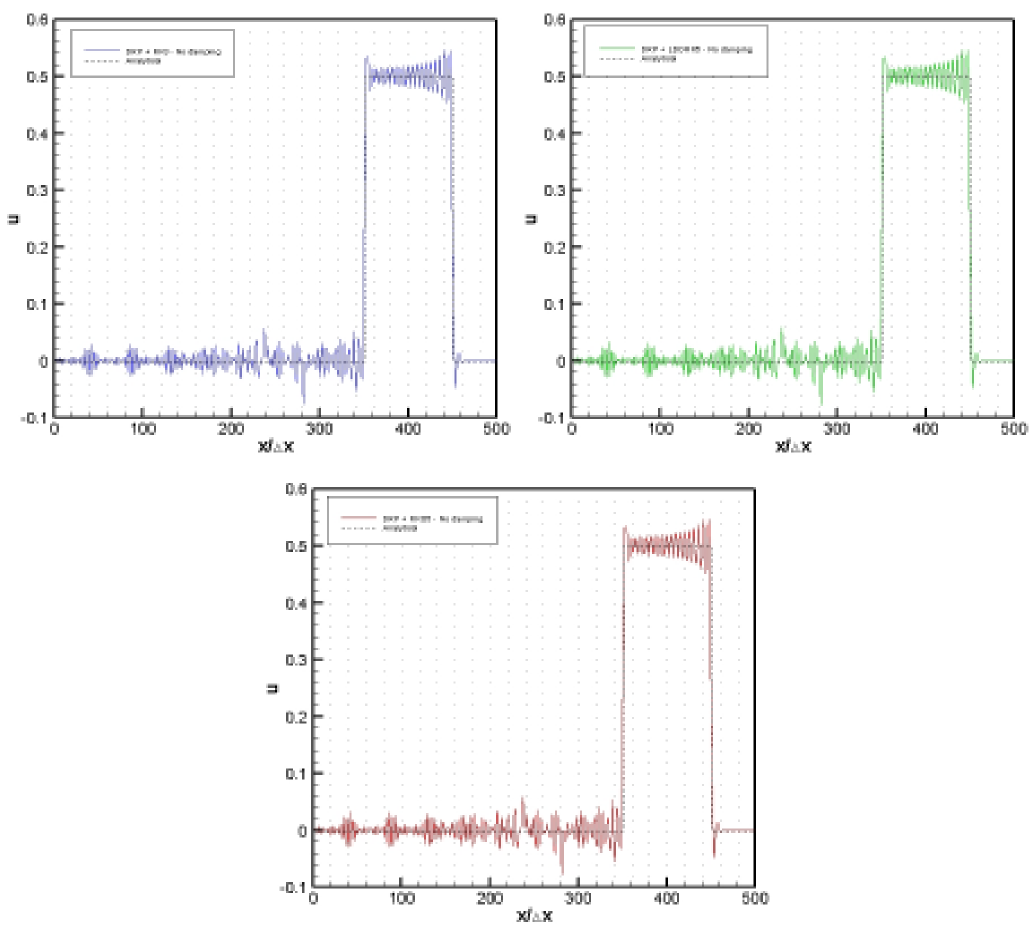

Figure 4. Comparison between the computed and the analytical solutions of the one-dimensional wave equation for the Box-car initial disturbance

The effect of the artificial selective damping terms in the wave equation can be clearly seen in Figure 5. Almost all the spurious oscillations were damped out. To obtain these results a damping constant of 0.3 was used. This value was selected based on the work of Roeck (2004). A larger value of this constant adds more damping into the scheme making the spurious waves smaller.

Even with the artificial selective damping it can be seen some overshoot in the left corner of the discontinuity. This overshoot is completely removed by increasing the value of the damping constant to 0.9 – Figure 6. However, the corners of the step have been smeared.

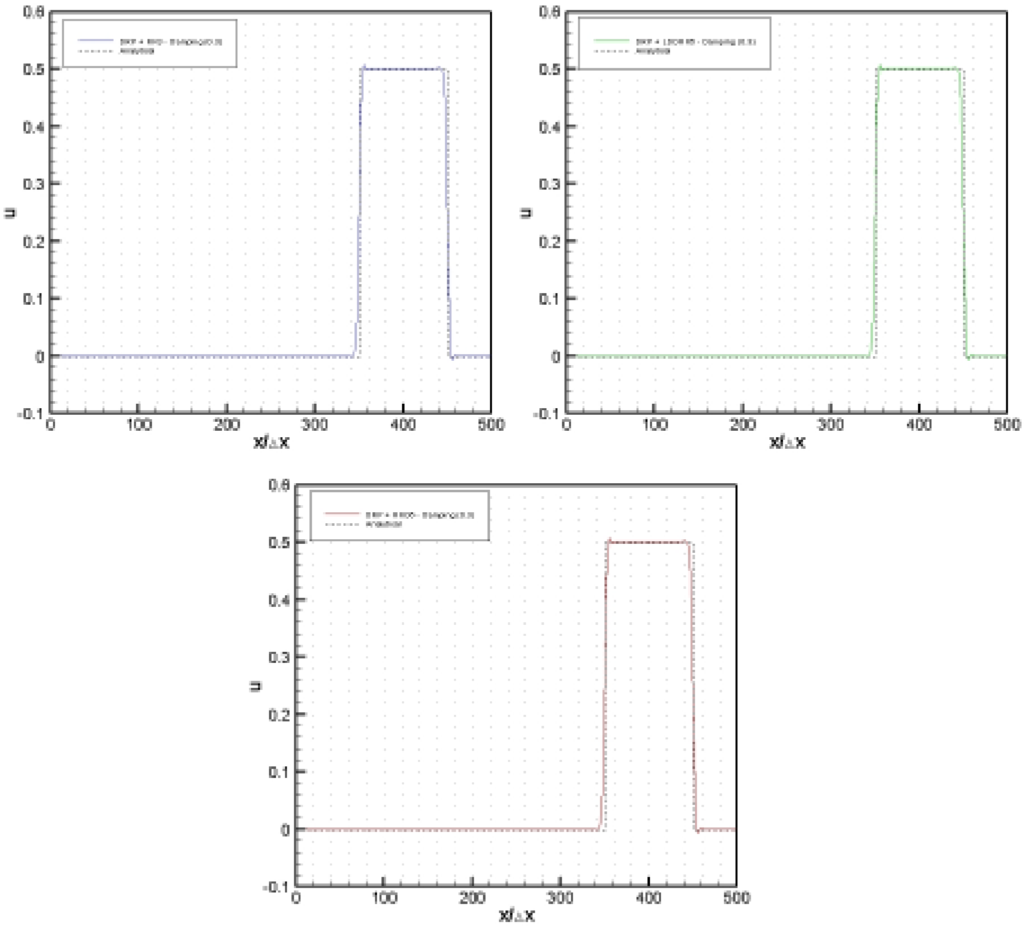

Figure 5. Effect of the damping function in the propagation of the Box-car function (damping constant of 0.3)

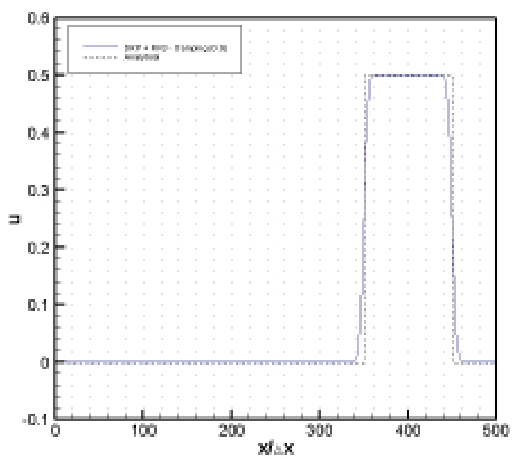

Figure 6. Effect of the damping function in the propagation of the Box-car function (damping constant of 0.9)

Contrary to the work of Roeck (2004), the increase of the damping constant over 0.7 did not bring any instability to the numerical scheme and the solution shown in Figure 6 could be obtained.

Figure 7 and 8 shows the numerical results for the propagation of the box-car function with the 15-point DRP scheme and the 9-point optimized central difference scheme of Bogey et al. (2002) associated with different Runge-Kutta schemes. For both schemes no artificial selective damping was applied. Even without damping, it's possible to see that the spatial discretization with more points perform better than the DRP 7-point scheme for the waves behind the pulse. However, at the discontinuity there is more overshoot.

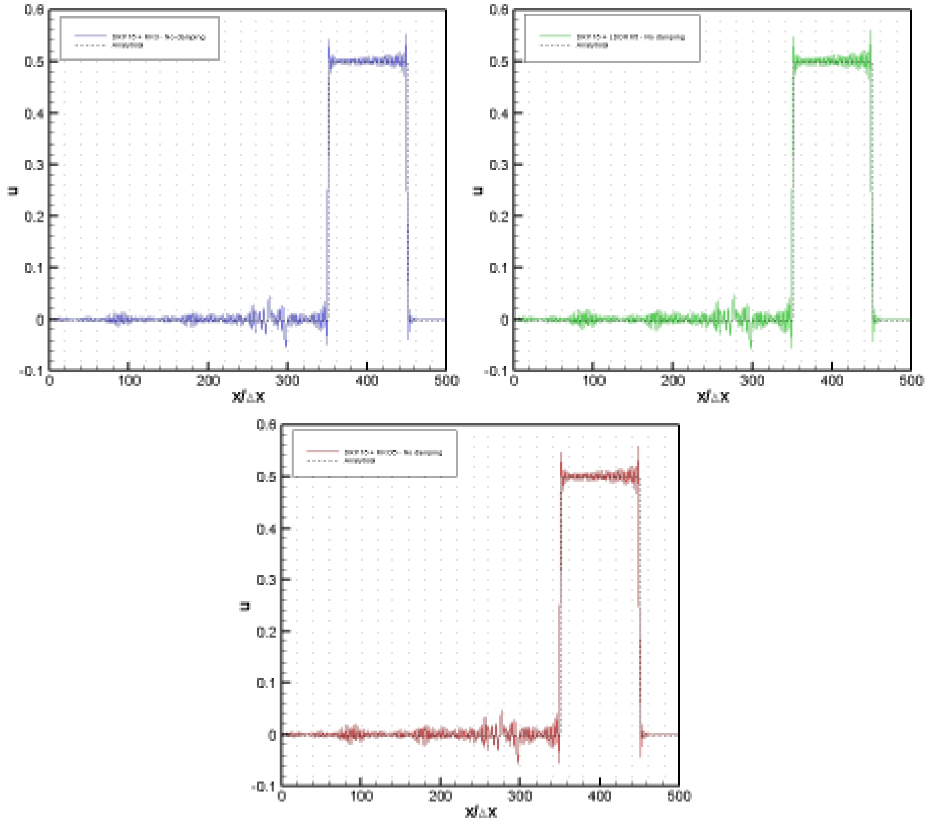

Figure 7. Propagation of Box-car function with 15-point DRP scheme – no artificial selective damping.

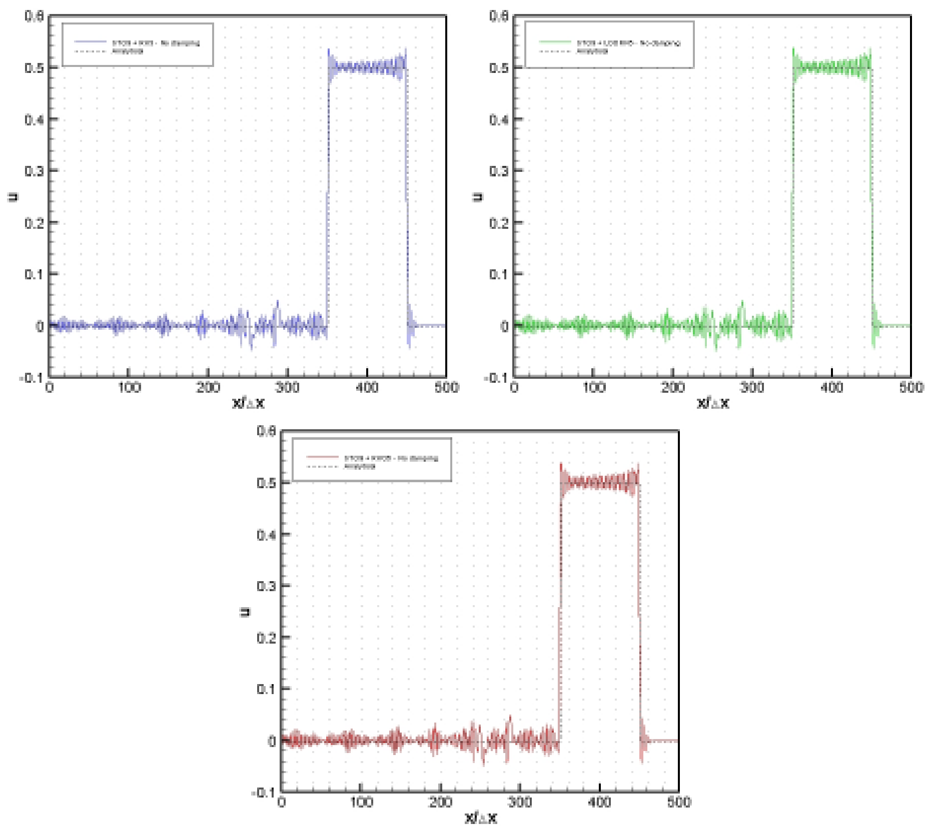

Figure 8. Propagation of Box-car function with 9-point optimized central-difference scheme – no artificial selective damping.

4.2 Initial Disturbance Function - Gaussian

Figure 9 shows the computed results of the seven-point DRP scheme with different Runge-Kutta time integration methods for the propagation of the Gaussian disturbance. In spite of the good agreement with the analytical solution some dispersed waves can be seen behind the pulse. These waves are originated by high-frequency components that are propagating at a lower wavespeed. It was expected that the low dispersion of the DRP scheme could diminish the amplitude of these trailing waves. However they are still present for the 7-point DRP scheme. It is important to emphasize again that the time integration schemes are almost not contributing to the numerical error since the stability range was satisfied with the Courant number. The main error is then introduced by the spatial difference scheme.

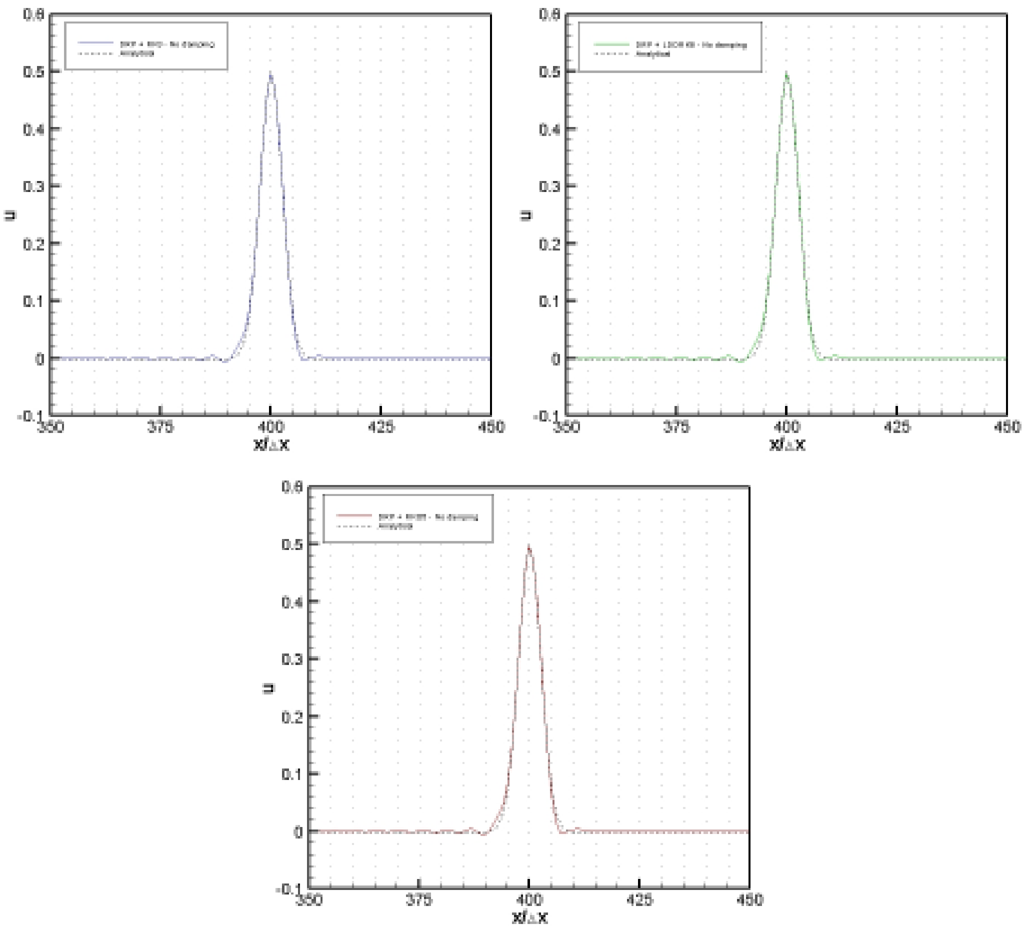

Figure 9. Propagation of Gaussian function with 7-point DRP scheme – no artificial selective damping.

The same calculations were done by increasing the stencil of the spatial discretization for 15 points using DRP schemes and for 9 points using an optimized central difference scheme - Figure 10 and 11 respectively. The increase in the number of points for the spatial discretization and the better dispersion properties of these schemes led to very good agreement for the pulse propagation when compared to the analytical solution. Practically, all the trailing waves were removed and the pulse was propagated correctly with the constant wave speed.

Both 15-point (DRP) and 9-point (STO9) schemes had a better performance when compared to the 7-point (DRP) scheme. However, these schemes are computationally more expensive due to a stencil with more points.

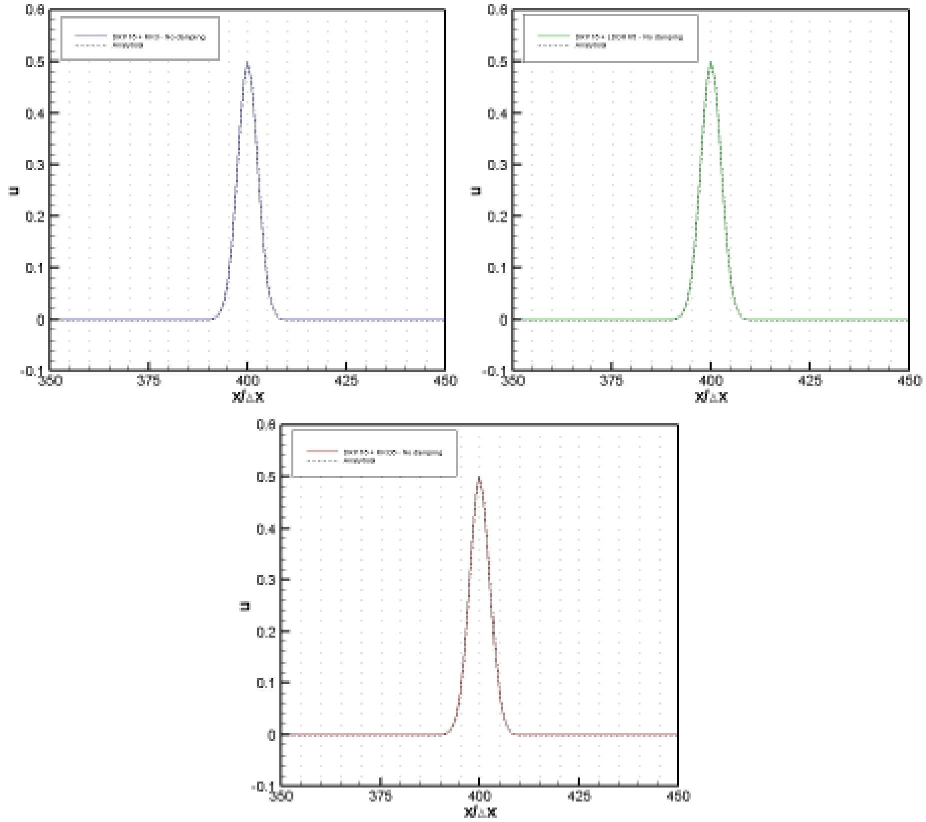

Figure 10. Propagation of Gaussian function with 15-point DRP scheme – no artificial selective damping.

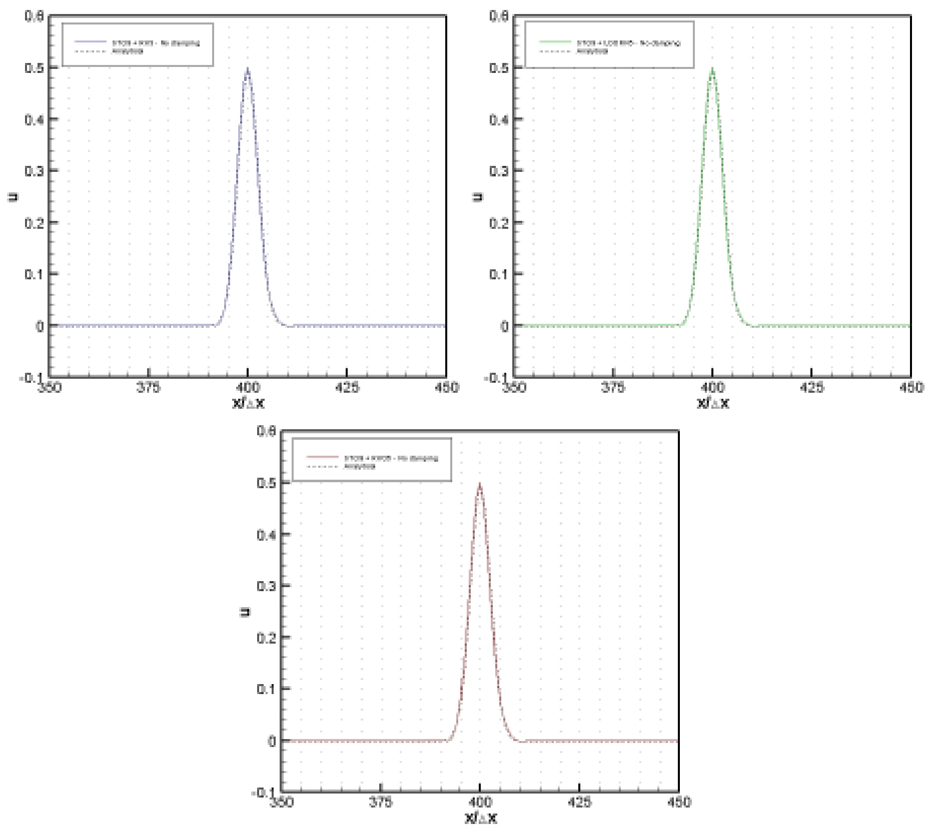

Figure 11. Propagation of Gaussian function with 9-point optimized central-difference scheme – no artificial selective damping.

5. Conclusions

The present work provided an overview of different spatial and temporal schemes that can be used for aeroacoustics calculation. Since, spatial and temporal discretization schemes with low-dispersion and low-dissipation properties have shown good performance in wave propagation problems it was investigated the DRP schemes and Runge-Kutta time integration methods which such properties. The DRP schemes with 7-point, 15-point and an optimized 9-point central difference scheme were evaluated for spatial discretization in the solution of a one-dimensional wave equation considering different initial disturbance propagation. To advance the solution in time, three different Runge-Kutta schemes were evaluated.

In general, the DRP schemes showed a good performance for wave propagation mainly due to the low dissipation and low dispersion properties. The 15-point DRP scheme was much more efficient than the 7-point, however the computational time increased. Also, the optimized 9-point central difference scheme presented good performance and it was better than the 7-point DRP scheme. The use of artificial selective damping was important to propagate the Box-car function correctly and to eliminate the spurious waves present in the solution. By increasing the damping constant, it was possible to reach a reasonable solution, but still with some smearing of the discontinuity.

Regarding the Runge-Kutta schemes, it's possible to say that over the range of stability, all the three schemes performed very well no bringing dispersion and dissipation to the solution. However, it's important to keep in mind that the schemes LDDRK5 and RKO5 are computationally more time consuming since at each stage evaluations of the spatial derivative need to be performed.

As a final recommendation of this work, the combination of the 9-point central difference (STO9) and the 15-point (DRP) scheme with the Runge-Kutta RKO5 is a good approach to initiate aeroacoustic computations.

6. Acknowledgement

The authors would like to thank EMBRAER (Empresa Brasileira de Aeronáutica – S.A) for the possibility of participation in this event.

7. References

Berland, J., Bogey, C., Bailly, C., "Low-dissipation and low-dispersion fourth-order Runge-Kutta algorithm", Computers & Fluids, 2005.

Bogey C., Bailly, C., "A family of low dispersive and low dissipative explicit schemes for computing the aerodynamic noise", AIAA-paper 2509, 2002.

Bogey C., Bailly, C., "A family of low-dispersive and low-dissipative explicit schemes for flow noise and noise computations", Journal of Computational Physics, 2004, 194, pp. 194-214.

Hu, F. Q., Hussaini, M. Y., Manthey, J. L., "Low-dissipation and low-dispersion Runge-Kutta schemes for computational aeroacoustics", Journal of Computational Physics, 124, 1996, pp. 177-191.

Lele, S. K., "Compact finite difference schemes with spectral-like resolution", Journal of Computational Physics, 1992, pp-16-42.

Lighthill M. J., "On sound generated aerodynamically", I, General Theory, Proceedings of Royal Society, London Ser., A221:564-87.

Roeck, W. De., Desmet, W., Baelmans, M., Sas, P.,2004, "An overview of high-order finite difference schemes for computational aeroacoustics", Proceedings of ISMA, pp. 353-368.

Tam, C. K., "Computational aeroacoustics: An overview of computational challenges and applications", International Journal of Computational Fluid Dynamics, Vol 18 (6), Aug 2004, pp. 547-567.

Tam, C. K., "Computational aeroacoustics: Issues and Methods", AIAA Journal, Vol 33 (10), October 2005, pp. 1788-1796.

Tam, C. K., Webb, J. C., "Dispersion-relation-preserving finite difference schemes for computational acoustics", Journal of Computational Physics, 107, 1993b, pp. 262-281.

Tam, C. K., Webb, W., Dong, J. C., "A study of short wave components in computational acoustics", Journal of Computational Acoustics, Vol 1, March 1993a, pp. 1-30.

Williamson, J. H., "Low-storage Runge-Kutta Schemes", Journal of Computational Physics, 35, 1980, pp. 48-56.

8. Copyright Notice